



ChemComm

Electrostatically-gated molecular rotors

Journal:	<i>ChemComm</i>
Manuscript ID	CC-COM-01-2022-000512.R2
Article Type:	Communication

SCHOLARONE™
Manuscripts

COMMUNICATION

Electrostatically-gated molecular rotors

Binzhou Lin,^a Ishwor Karki,^a Perry J. Pellechia^a and Ken D. Shimizu*^aReceived 00th January 20xx,
Accepted 00th January 20xx

DOI: 10.1039/x0xx00000x

The ability to control molecular-scale motion using electrostatic interactions was demonstrated using an *N*-phenylsuccinimide molecular rotor with an electrostatic pyridyl-gate. Protonation of the pyridal-gate forms stabilizing electrostatic interactions in the transition state of the bond rotation process that lowers the rotational barrier and increases the rate of rotation by two orders of magnitude. Molecular modeling and energy decomposition analysis confirms the dominant role of attractive electrostatic interactions in lowering the bond rotation transition state.

The development and study of synthetic molecular devices and molecular machines are an exciting new area of research.^{1–5} An important challenge in the field is developing effective methods of controlling molecular-scale motion using macroscale inputs and stimuli. For example, stimuli used to control the rates of rotation of molecular rotors have included: light,^{6–11} metal ions,^{12–14} hydrogen bonds,^{15–17} redox,^{18–20} anions,²¹ guests,^{16,22,23} and protons.^{24–29} The majority of these systems were molecular brakes where the stimuli slowed the rate of rotation. More rare were stimuli that increased or accelerated the rate of rotations.^{15,19,29,20,27,28}

In this work, we demonstrate the use of attractive electrostatic interactions to stabilize transition states, lower barriers, and increase rates of molecular scale motion. The control of molecular-scale motion using electrostatic interactions has the potential of being integrated with existing micro- and nanoscale devices such as memory and transistors that are electrically addressed and controlled.³⁰ In addition, the electrostatic gating mechanism could be coupled with electron microscopy methods that can manipulate and investigate the electronic states of single molecules.^{31–34}

Electrostatic interactions have been employed to control the thermodynamic equilibria of molecular devices by stabilizing or destabilizing one or more possible states.^{1,35} However, there are few examples that use electrostatic interactions to control the kinetics and rates of molecular motion. The examples we did find used repulsive electrostatic interactions to raise barriers such as preventing pseudorotaxane dethreading.³⁶ Therefore, the goal of this work was to develop a molecular device in which attractive electrostatic interactions lower barriers and increase the rate of molecular motion by forming stabilizing transition state interactions.

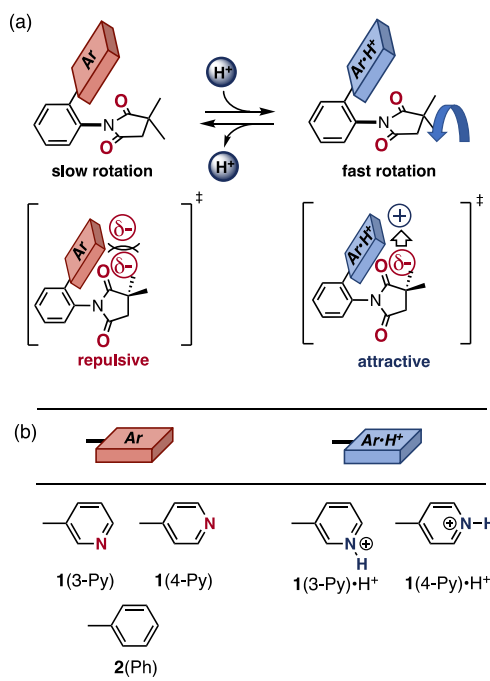


Fig 1 a) Schematic representation of the electrostatically-gated rotors **1** which are activated by protonation that lowers the rotational barriers by forming attractive electrostatic interactions in the bond rotation TS and b) chart of the chemical structures of **1**, **1•H⁺**, and control rotor **2**.

^a Department of Chemistry and Biochemistry, University of South Carolina, Columbia, SC 29208, USA. Email: shimizu@mailbox.sc.edu.

† Footnotes relating to the title and/or authors should appear here.

Electronic Supplementary Information (ESI) available: [details of any supplementary information available should be included here]. See DOI: 10.1039/x0xx00000x

A challenge in demonstrating electrostatically controlled increases in molecular-scale motion is separating the electrostatic component from other TS interactions in particular the steric interactions. Our recent studies of C=O... π (phenyl) interactions using molecular rotors suggested a possible solution.³⁷ The substituents on the phenyl gates only modulated the electrostatic interaction as the steric component stayed constant. Thus, in the design of the electrostatically gated rotors **1**, a structurally similar 3- and 4-pyridyl gate was used as the protonation of the pyridyl group would provide larger changes in the electrostatic interactions due to the presence of the positive charge with minimal change in the steric interactions.

The electrostatically gated molecular rotors are based on the *N*-phenylimide framework, which displays restricted rotation about the central C-N single bond.^{16,38,39} Rotors **1**(3-Py) and **1**(4-Py) have 3- or 4-pyridyl electrostatic gates appended to the *ortho*-position of the *N*-phenyl stator. The electrostatically negative π -face of the neutral pyridyl groups form repulsive electrostatic interactions with the imide C=O oxygen in the bond rotation transition state leading to a high barrier and slow rotation of the succinimide rotor (Fig. 1a). However, when the pyridyl gate is protonated in **1**(3-Py)•H⁺ and **1**(4-Py)•H⁺, the positively charged pyridinium group forms attractive electrostatic interactions with the imide C=O oxygen lowering the barrier and speeding up rotation of the succinimide rotor. A control rotor **2**(Ph) was also prepared with a phenyl gate, which lacks a basic pyridyl nitrogen and thus cannot be protonated.

Rotors **1** and **2** were synthesized via the thermal condensation of 3,3-dimethylsuccinic anhydride and an *ortho*-substituted aniline (AcOH, 140 °C, 24 h).⁴⁰ The dimethyl groups break the symmetry of the succinimide rotor, enabling the rate of rotation to be monitored by ¹H NMR. For example, the succinimide CH₂ protons were diastereotopic in the unprotonated rotors **1**(3-Py), **1**(4-Py), and **2**(Ph), due to slow rotation around the C-N bond at (25 °C) (Fig. 2, 0 eq. MsOH). However, when the pyridyl groups are protonated with methane sulfonic acid (MsOH), the succinimide CH₂ protons were in fast exchange and collapsed into a singlet due to fast rotation around the C-N bond (Fig. 2a). By comparison, the ¹H NMR spectra of control rotor **2**(Ph) did not change when MsOH was added. The diastereomeric succinimide CH₂ protons shifted downfield but remained in slow exchange (Fig. 2b).

The differences in the rates of rotation and rotational barriers were observed by the changes in coalescence temperatures (Fig. S12) and quantitatively measured using EXSY NMR (Table 1). The changes in rotational barrier were consistent with the ability of the pyridinium gates to electrostatically lower the rotational barriers of rotors **1**. Initially, the neutral rotors **1**(3-Py), **1**(4-Py), and **2**(Ph) had similar barriers of 18.8 to 20.6 kcal/mol. On the addition of 3 equivalents of MsOH, the rotational barriers of the pyridyl rotors, **1**(3-Py) and **1**(4-Py) decreased by 2.1 and 3.2 kcal/mol. In contrast, the rotational barrier for the control rotor **2**(Ph) increased slightly on addition of MsOH. The changes in barriers correspond to increases in the rates of rotation of 32 and 206 fold for rotors **1**(3-Py)•H⁺ and **1**(4-Py)•H⁺ respectively.

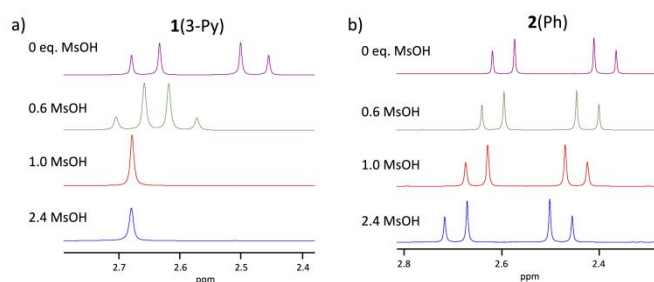


Fig 2. ¹H NMR spectra of the succinimide CH₂ protons for a) electrostatically gated rotor **1**(3-Py) and b) control rotor **2**(Ph) with increasing number of equivalents of MsOH. The ¹H NMR spectra for **1**(4-Py) were similar to those of **1**(3-Py).

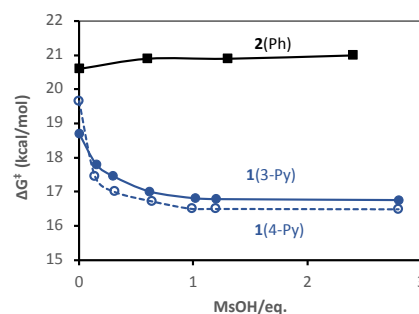


Fig 3. Rotational barriers for rotors **1**(3-Py), **1**(4-Py), and **2**(Ph) with increasing equivalents of methanesulfonic acid (MsOH) in TCE-d₂ as measured by EXSY ¹H NMR.

To verify that attractive electrostatic interactions were the reason for the lower barriers of the pyridinium rotors, the geometries, rotational barriers, and energy decomposition analyses were calculated. The ground state and TS geometries (B3LYP-D3/6-311G* with a solvent dielectric of 8.42 for TCE) were very similar for the unprotonated and protonated rotors **1** and control rotor **2**. In particular, the TS structures were nearly identical as shown in Fig. 4 with the C=O groups pointing into the π -face of the perpendicular aryl rings. The closest contacts from the oxygen of the C=O to the aryl rings were also very similar (2.42 – 2.58 Å). Most importantly, the rigid framework and the perpendicular geometry of the pyridinium rings prevent the N-H protons of **1**(3-Py)•H⁺ and **1**(4-Py)•H⁺ from forming intramolecular hydrogen bonding interactions that could have provided another explanation for their lower barriers.

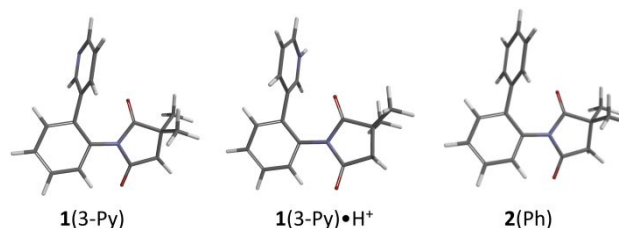


Fig 4. Calculated (B3LYP-D3/6-311G*) transition state structures for the unprotonated and protonated electrostatically gated rotor **1**(3-Py) and **1**(3-Py)•H⁺ and control rotor **2**(Ph).

The calculated rotational barriers ($\Delta G^{\ddagger}_{\text{calc}}$) from the GS and TS structures were also able to reproduce the experimentally observed lower rotational barriers of **1**(3-Py)•H⁺ and **1**(4-

Py)•H⁺ (Table 1).⁴¹ The average difference between the neutral and protonated rotors for the experimentally measured ($\Delta\Delta G_{\text{expt}}^{\ddagger}$) and calculated barriers ($\Delta\Delta G_{\text{calc}}^{\ddagger}$) were very similar (2.7 and 2.8 kcal/mol).

Table 1 Experimental and calculated rotational barriers and rates of rotations.

Rotor	$\Delta G_{\text{expt}}^{\ddagger}$ ^a (kcal/mol)	$\Delta G_{\text{calc}}^{\ddagger}$ ^b (kcal/mol)	rotation rate ^c (Hz)
1 (3-Py)	18.8	21.9 (20.7)	0.095
1 (4-Py)	19.7	20.1 (20.5)	0.025
1 (3-Py)•H ⁺	16.7 ^e	19.0 (13.8)	3.02
1 (4-Py)•H ⁺	16.5 ^e	17.5 (12.7)	5.14
2 (Ph)	20.6	20.9 (22.2)	0.0049

^a Rotational barriers measured by EXSY of the ¹H NMR in TCE-d₂. ^b Calculated using B3LYP-D3/6-311G* in 1,1,2,2-tetrachloroethane (dielectric = 8.42) at 298.15 K. Values in parentheses were calculated in the gas phase at 298.15 K. ^c Calculated using $\Delta G_{\text{expt}}^{\ddagger}$ for 298.15 K. ^e **1**(3-Py) and **1**(4-Py) were protonated by the addition of 3 equivalents of MsOH in TCE-d₂.

Comparisons of the barriers calculated in solvent (dielectric = 8.42) and the gas phase provided the first evidence for presence of stabilizing TS electrostatic interactions (Table 1). The neutral rotors **1**(3-Py), **1**(4-Py), and **2**(Ph) had similar $\Delta G_{\text{calc}}^{\ddagger}$ values in solvent and the gas phase. In contrast, the positively charged pyridinium rotors **1**(3-Py)•H⁺ and **1**(4-Py)•H⁺ had very different $\Delta G_{\text{calc}}^{\ddagger}$ values in solvent and the gas phase. The average change in the barrier ($\Delta\Delta G_{\text{calc}}^{\ddagger}$) on protonation for rotors **1** was small in solvent (-2.75 kcal/mol) and large (-7.35 kcal/mol) in the gas phase. These differences are consistent with the electrostatic interactions being screened in solvent, which reduces their effect on the rotational barriers.

Direct evidence for the stabilizing electrostatic TS interactions in the pyridinium rotors was provided by energy decomposition analyses of the non-covalent interactions in the transition states (Fig. 5). The intramolecular interaction energies between the imide carbonyl groups (C=O) and the aromatic pyridyl, pyridinium, and phenyl gates in the TS (B3LYP-D3/6-311G*) were calculated using the functional group interaction analysis method (fi-SAPT(0), jun-cc-pVZT).⁴² The calculated interaction energy trends mirrored the experimental rotational barrier trends. The neutral rotors, **1**(3-Py), **1**(4-Py), and **2**(Ph), had destabilizing C=O•••aryl interactions ($E_{\text{total}} = 11.7$ to 13.6 kcal/mol). Whereas, the positively charged rotors, **1**(3-Py)•H⁺, **1**(4-Py)•H⁺, had stabilizing interactions ($E_{\text{total}} = -4.4$ and -8.0 kcal/mol). The origins of the differences in the E_{total} values between the neutral and positively charged rotors were evident from an analysis of the component repulsion-exchange, electrostatic, induction, and dispersion (E_{exch} , E_{elec} , E_{ind} , and E_{disp}) terms. The E_{exch} , E_{elec} , and E_{disp} terms were similar between the neutral and positively charged rotors. In particular, the similarity in the repulsive E_{exch} terms provided confirmation that the pyridyl gates do not change in size on protonation or deprotonate. Only, the E_{elec} term changed dramatically between the neutral and protonated rotors **1**. For example, the change in the E_{elec} term (ΔE_{elec}) between **1**(3-Py) and **1**(3-Py)•H⁺ was -16.2 kcal/mol which was very similar to the differences in the total interaction energies ($\Delta E_{\text{total}} = -17.1$ kcal/mol). Likewise,

the ΔE_{elec} (-18.3 kcal/mol) and ΔE_{total} (109.8 kcal/mol) terms were very similar for **1**(4-Py) and **1**(3-Py)•H⁺. The electrostatic nature of the intramolecular C=O••• π (pyridyl) are consistent with our recent study, which found that stabilizing C=O••• π (phenyl) interactions in neutral aromatic systems were dominated by electrostatic interactions.³⁷ Additional SAPT analyses were conducted that included the intramolecular interactions of the pyridyl/pyridinium group in the ground state and transition state (Fig. S13), leading to the same conclusion. The electrostatic interactions were the dominant term in the change in barrier on protonation and deprotonation of the pyridyl gate.

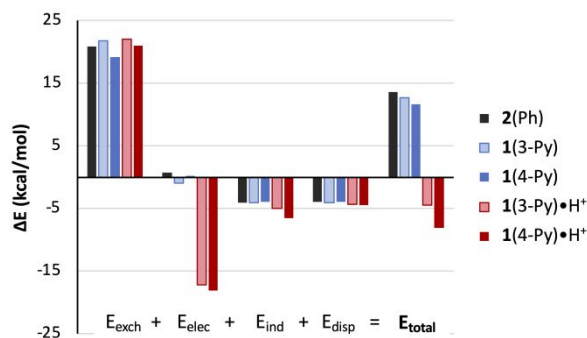


Fig 5 The fi-SAPT (SAPT(0), jun-cc-pVZ) energies for the intramolecular C=O•••aryl interactions in the optimized TS structures (B3LYP-D3, 6-311G*) for protonated and unprotonated rotors **1** and control rotor **2**.

Finally, the reversibility of the electrostatic gates were demonstrated by following four protonation-deprotonation cycles using ¹H NMR lineshape analysis at 25 °C (Fig. S11). In each cycle, the rotor **1**(3-Py) in TCE-d₂ was treated with 3 equivalents of MsOH followed by neutralization by washing aqueous NaHCO₃ solutions. The rotor cleanly switched from slow-exchange to fast-exchange and back to slow-exchange without degradation or formation of by-products.

Conclusions

Molecular pyridyl rotor **1** was designed in which the rate of rotation is accelerated by the formation of attractive through-space electrostatic interactions. Protonation of the pyridyl gates on the stator leads to a positively charged pyridinium aromatic surface that forms stabilizing electrostatic interactions with the electrostatically negative C=O oxygen in the bond rotation transition state. Dynamic NMR and theory concurred that the pyridinium rotors **1**(3-Py)•H⁺ and **1**(4-Py)•H⁺ had rotational barriers that were 2.7 to 2.8 kcal/mol lower than the neutral pyridyl rotors **1**(3-Py) and **1**(4-Py), leading to increases in the rates of rotation of 32 and 206 times. Computational modelling and energy decomposition analysis were consistent with the formation of stabilizing electrostatic interactions in the TS between the face of the pyridinium gate and the C=O oxygens in **1**(3-Py)•H⁺ and **1**(4-Py)•H⁺. Similar attractive through-space electrostatic interactions have recently been demonstrated to be able to control the thermodynamic equilibrium of conformationally

flexible molecules,^{43,44} contribute to aromatic interactions,⁴⁵ and have also been hypothesized to play a key role in the kinetic rate enhancement of biological⁴⁶ and synthetic processes.^{47–49} Thus, this study demonstrates that stabilizing through-space electrostatic interactions can also be used to control and accelerate molecular-scale motion.

Conflicts of interest

There are no conflicts to declare.

Acknowledgements

This work was supported by the National Science Foundation grant CHE 2003889.

Notes and references

- S. Erbas-Cakmak, D. A. Leigh, C. T. McTernan and A. L. Nussbaumer, *Chem. Rev.*, 2015, **115**, 10081–10206.
- I. Aprahamian, *ACS Cent. Sci.*, 2020, **6**, 347–358.
- D. R. S. Pooler, A. S. Lubbe, S. Crespi and B. L. Feringa, *Chem. Sci.*, 2021, **12**, 14964–14986.
- J. Dong, V. Wee, S. B. Peh and D. Zhao, *Angew. Chem.*, 2021, **133**, 16415–16428.
- V. Balzani, A. Credi, F. M. Raymo and J. F. Stoddart, *Angew. Chem.-Int. Ed. Engl.*, 2000, **39**, 3349–3391.
- J. S. Yang, Y. T. Huang, J. H. Ho, W. T. Sun, H. H. Huang, Y. C. Lin, S. J. Huang, S. L. Huang, H. F. Lu and I. Chao, *Org. Lett.*, 2008, **10**, 2279–2282.
- M. C. Basheer, Y. Oka, M. Mathews and N. Tamaoki, *Chem. - Eur. J.*, 2010, **16**, 3489–3496.
- W. T. Sun, S. L. Huang, H. H. Yao, I. C. Chen, Y. C. Lin and J. S. Yang, *Org. Lett.*, 2012, **14**, 4154–7.
- W. S. Tan, P.-Y. Chuang, C.-H. Chen, C. Prabhakar, S.-J. Huang, S.-L. Huang, Y.-H. Liu, Y.-C. Lin, S.-M. Peng and J.-S. Yang, *Chem. - Asian J.*, 2015, **10**, 989–997.
- T. van Leeuwen, W. Danowski, S. F. Pizzolato, P. Štacko, S. J. Wezenberg and B. L. Feringa, *Chem. - Eur. J.*, 2018, **24**, 81–84.
- R. Asato, C. J. Martin, S. Abid, Y. Gisbert, F. Asanoma, T. Nakashima, C. Kammerer, T. Kawai and G. Rapenne, *Inorg. Chem.*, 2021, **60**, 3492–3501.
- T. R. Kelly, M. C. Bowyer, K. V. Bhaskar, D. Bebbington, A. Garcia, F. R. Lang, M. H. Kim and M. P. Jette, *J. Am. Chem. Soc.*, 1994, **116**, 3557.
- R. Annunziata, M. Benaglia, M. Cinquini, L. Raimondi and F. Cozzi, *J. Phys. Org. Chem.*, 2004, **17**, 749–751.
- Y. Wu, G. Wang, Q. Li, J. Xiang, H. Jiang and Y. Wang, *Nat. Commun.*, DOI:10.1038/s41467-018-04323-4.
- I. Alfonso, M. I. Bргуete and S. V. Luis, *J. Org. Chem.*, 2006, **71**, 2242–2250.
- G. Rushton, E. C. Vik, W. G. Burns, R. D. Rasberry and K. D. Shimizu, *Chem. Commun.*, 2017, **53**, 12469–12472.
- Z.-F. Liu, X. Chen, Z. F. Mou and W. J. Jin, *J. Mater. Chem. C*, 2020, **8**, 16100–16106.
- P. V. Jog, R. E. Brown and D. K. Bates, *J. Org. Chem.*, 2003, **68**, 8240–3.
- C. H. Yang, C. Prabhakar, S. L. Huang, Y. C. Lin, W. S. Tan, N. C. Misra, W. T. Sun and J. S. Yang, *Org. Lett.*, 2011, **13**, 5632–5635.
- G. Chen and Y. Zhao, *Org. Lett.*, 2014, **16**, 668–671.
- S. Han, Y. Wu, R. Duan, H. Jiang and Y. Wang, *Asian J. Org. Chem.*, 2019, **8**, 83–87.
- A. Comotti, S. Bracco, P. Valsesia, M. Beretta and P. Sozzani, *Angew. Chem. Int. Ed.*, 2010, **49**, 1760–1764.
- S. Bracco, T. Miyano, M. Negroni, I. Bassanetti, L. Marchio', P. Sozzani, N. Tohnai and A. Comotti, *Chem. Commun.*, 2017, **53**, 7776–7779.
- K. Nikitin, H. Mueller-Bunz, Y. Ortin and M. J. McGlinchey, *Chem. - Eur. J.*, 2009, **15**, 1836–1843.
- D. Zhang, Q. Zhang, J. H. Sua and H. Tian, *Chem. Commun.*, 2009, 1700–1702.
- Y. Iwasaki, R. Morisawa, S. Yokojima, H. Hasegawa, C. Roussel, N. Vanthuyne, E. Caytan and O. Kitagawa, *Chem. - Eur. J.*, 2018, **24**, 4453–4458.
- Y. Suzuki, M. Kageyama, R. Morisawa, Y. Dobashi, H. Hasegawa, S. Yokojima and O. Kitagawa, *Chem. Commun.*, 2015, **51**, 11229–11232.
- H. Chen, X. Tang, H. Ye, X. Wang, H. Zheng, Y. Hai, X. Cao and L. You, *Org. Lett.*, 2021, **23**, 231–235.
- B. E. Dial, P. J. Pellechia, M. D. Smith and K. D. Shimizu, *J. Am. Chem. Soc.*, 2012, **134**, 3675–3678.
- D. Xiang, X. Wang, C. Jia, T. Lee and X. Guo, *Chem. Rev.*, 2016, **116**, 4318–4440.
- M. Tsutsui and M. Taniguchi, *Sensors*, 2012, **12**, 7259–7298.
- H. Stahlberg and T. Walz, *ACS Chem. Biol.*, 2008, **3**, 268–281.
- C. Ni and J.-Z. Wang, *Surf. Rev. Lett.*, 2018, **25**, 1841004.
- G. J. Simpson, V. García-López, A. Daniel Boese, J. M. Tour and L. Grill, *Nat. Commun.*, 2019, **10**, 4631.
- J. F. Stoddart, *Angew. Chem. Int. Ed.*, 2017, **56**, 11094–11125.
- Y. Qiu, B. Song, C. Pezzato, D. Shen, W. Liu, L. Zhang, Y. Feng, Q.-H. Guo, K. Cai, W. Li, H. Chen, M. T. Nguyen, Y. Shi, C. Cheng, R. D. Astumian, X. Li and J. F. Stoddart, *Science*, 2020, **368**, 1247–1253.
- E. C. Vik, P. Li, D. O. Madukwe, I. Karki, G. S. Tibbetts and K. D. Shimizu, *Org. Lett.*, 2021, **23**, 8179–8182.
- K. Kishikawa, K. Yoshizaki, S. Kohmoto, M. Yamamoto, K. Yamaguchi and K. Yamada, *J. Chem. Soc. Perkin 1*, 1997, 1233–1239.
- E. Kumarasamy, R. Raghunathan, M. P. Sibi and J. Sivaguru, *Chem. Rev.*, 2015, **115**, 11239–300.
- P. Li, E. C. Vik and K. D. Shimizu, *Acc. Chem. Res.*, 2020, **53**, 2705–2714.
- E. C. Vik, P. Li, P. J. Pellechia and K. D. Shimizu, *J. Am. Chem. Soc.*, 2019, **141**, 16579–16583.
- T. M. Parker, L. A. Burns, R. M. Parrish, A. G. Ryno and C. D. Sherrill, *J. Chem. Phys.*, 2014, **140**, 094106.
- R. J. Burns, I. K. Mati, K. B. Muchowska, C. Adam and S. L. Cockroft, *Angew. Chem. Int. Ed.*, 2020, **59**, 16717–16724.
- J. Hwang, P. Li, E. C. Vik, I. Karki and K. D. Shimizu, *Org. Chem. Front.*, 2019, **6**, 1266–1271.
- S. E. Wheeler and K. N. Houk, *J. Chem. Theory Comput.*, 2009, **5**, 2301–2312.
- A. Warshel, P. K. Sharma, M. Kato, Y. Xiang, H. Liu and M. H. M. Olsson, *Chem. Rev.*, 2006, **106**, 3210–3235.
- S. Shaik, R. Ramanan, D. Danovich and D. Mandal, *Chem. Soc. Rev.*, 2018, **47**, 5125–5145.
- Y.-Y. Xing, S.-S. Chen, D.-Z. Chen and D. J. Tantillo, *Phys. Chem. Chem. Phys.*, 2020, **22**, 26955–26960.
- Y. Zhao, Y. Cotellet, L. Liu, J. López-Andarias, A.-B. Bornhof, M. Akamatsu, N. Sakai and S. Matile, *Acc. Chem. Res.*, 2018, **51**, 2255–2263.